photonics

MDPI

Article

Dispersion Analysis and Control in a Yb-Doped Fiber Chirped Pulse Amplification System and Second-Harmonic Generation

Zhengying You [1,2], Qian Wang [1,2], Yuanyuan Fan [1,2,*], Yifan Zhao [1,2], Yan Qi [1,2], Boxia Yan [1,2], Ning Wen [1,2], Zhe Han [1,2], Mi Zhou [1,2] and Yanwei Wang [1,2]

[1] Institute of Microelectronics of the Chinese Academy of Sciences, Beijing 100029, China; youzhengying23@mails.ucas.ac.cn (Z.Y.)
[2] University of Chinese Academy of Sciences, Beijing 100049, China
* Correspondence: fanyuanyuan@ime.ac.cn

Abstract

We report a dispersion-controlled Yb-doped fiber chirped pulse amplification (CPA) system incorporating a tunable chirped fiber Bragg grating (CFBG) stretcher and a single-grating transmission compressor for dynamic compensation of power-dependent nonlinear effect. During the pulse amplification, the CFBG introduces adjustable third-order dispersion (TOD). By tuning the initial TOD provided by CFBG from −0.1965 ps³ at 2.37 W to −0.1791 ps³ at 9.65 W, residual TOD is efficiently compensated with the power-dependent nonlinear effect. As a result, by optimizing the dispersion balance at each output power, nearly constant femtosecond pulses with a duration of 250 fs are obtained over the entire power range, confirming effective control of nonlinear and dispersive effects in the amplification. The high-quality 1030 nm pulses enable efficient second-harmonic generation (SHG) in a type-I BBO crystal, producing 3.56 W femtosecond output at around 515 nm with a pulse duration of 190 fs, close to the Fourier transform limit. These results demonstrate a robust approach to generating high-power and temporal coherent ultrafast pulses suitable for precision micromachining and two-photon polymerization.

Keywords: chirped pulse amplification; Yb-doped fiber; femtosecond laser; optical harmonic generation

1. Introduction

Femtosecond laser sources have become indispensable tools in ultrafast science and technology because their extremely short pulse durations combine high peak power with fine temporal resolution, enabling applications such as laser direct writing, biomedical imaging, precision micromachining, and optical frequency comb generation [1]. Among these applications, Yb-based femtosecond systems operating near 1030 nm have unlocked new opportunities for high-repetition-rate, high-flux nonlinear spectroscopy and imaging [2]. Meanwhile, the frequency-doubled counterpart at 515 nm is particularly well-suited for two-photon polymerization (TPP) owing to its enhanced absorption cross-section in photoresists, enabling sub-micrometer structuring and high-precision surface patterning [3].

Although various approaches have been explored for power and energy scaling of femtosecond fiber oscillators, the most effective strategy remains the chirped pulse amplification (CPA) scheme, in which low energy seed pulses are temporally stretched, amplified, and subsequently recompressed. As the output power of the fiber CPA system increases, nonlinear effects including self-phase modulation (SPM) [4], self-steepening [5],

Check for updates

Received: 24 December 2025
Revised: 10 January 2026
Accepted: 12 January 2026
Published: 27 January 2026

Copyright: © 2026 by the authors. Licensee MDPI, Basel, Switzerland. This article is an open access article distributed under the terms and conditions of the Creative Commons Attribution (CC BY) license.

and stimulated Raman scattering [6] become significant and distort both the temporal and spectral characteristics of the pulse. SPM stands as the dominant Kerr nonlinearity in ultrashort pulse propagation, causing significant spectral broadening and undesirable phase distortions, which can either degrade or partially compensate dispersion-induced distortions depending on its magnitude and sign of residual higher-order phase. At the same time, incomplete compensation of group delay dispersion (GDD) and third-order dispersion (TOD) accumulated in the stretcher, amplifier, and compressor can result in residual chirp and prevents the pulse from being fully compressed [7]. In high-power CPA systems, the interplay between nonlinear phase accumulation and residual high-order dispersion becomes the dominant factor that limits the achievable pulse duration and pulse quality [8,9].

Recent studies have shown that the pulse compressibility of high-energy femtosecond fiber CPA systems is primarily governed by the interplay between accumulated nonlinear phase and third-order dispersion (TOD). Lv et al. (2016) reported that a mismatched TOD and nonlinear phase at different energies lead to pulse broadening, whereas partial self-compensation between them enables shorter pulses at moderate nonlinear phase levels [10]. Song et al. (2017) further demonstrated that introducing negative TOD pre-compensation, combined with controlled SPM, allows the generation of high-energy pulses that compress close to the transform limit of 280 fs at a single pulse output of 10.4 μJ [9]. Wei et al. (2020) also used mismatched negative TOD to counteract nonlinear phase in an Er-doped CPA system, achieving sub 400 fs pulses in an all-fiber configuration [11]. More recently, Wang et al. (2023) employed cascaded CFBGs to finely tune higher-order dispersion, enabling sub-picosecond compression even at several hundred watts of average power [12]. Overall, these studies confirm that effective pulse compression at high power requires precise balancing of TOD and nonlinear effect, and that GDD compensation alone is insufficient, highlighting the need for flexible, tunable dispersion management approaches. Moreover, the stability and compressibility of the fundamental pulse directly affect the quality of second-harmonic pulses, making dispersion-optimized amplification crucial for efficient and high-quality SHG at 515 nm.

To address these limitations, we develop a Yb-doped fiber CPA system incorporating a tunable chirped fiber Bragg grating (CFBG) that provides adjustable GDD and TOD, enabling dynamic compensation of the power-dependent nonlinear phase accumulated in the amplifier. By carefully optimizing the stretcher amplifier and compressor dispersion balance and introducing a pre-chirp control, the system maintains nearly constant pulse duration over a wide range of output powers. At the maximum compressed output of 9.65 W, the pulse duration remains as short as 250 fs, indicating that the interplay between controllable dispersion and nonlinear phase accumulation is effectively managed across the operating range. The high-quality 1030 nm pulses further enable efficient second-harmonic generation in a type-I BBO crystal, yielding 3.56 W of 515 nm femtosecond pulses with near transform-limited temporal characteristics. These results demonstrate that precise dispersion control combined with managed nonlinearity allows consistent pulse compression and efficient frequency doubling, offering a robust platform for high-power ultrafast applications such as two-photon polymerization and precision microfabrication.

2. Nonlinearity and Dispersion

In high-power fiber CPA systems, the temporal quality of the recompressed pulse is jointly determined by the accumulated nonlinear phase and the net dispersion of the stretcher amplifier and compressor chain. Among the nonlinear effects, SPM plays the

dominant role, imposing an intensity dependent phase shift during propagation through the gain medium. This nonlinear phase shift is typically expressed as follows [7]:

$$\phi_{NL} = \gamma P(z) L_{eff}, \tag{1}$$

where L_{eff} is the effective fiber length, γ is the fiber's nonlinear coefficient and $P(z)$ is the instantaneous pulse peak power at position z. It produces a frequency chirp that becomes increasingly significant as the pulse energy and peak power grow. The cumulative impact of SPM is conveniently quantified using the B-integral, representing the total accumulated nonlinear phase shift experienced by the peak of the pulse along the propagation length; it is mathematically defined as follows [13]:

$$\mathrm{B} = \int_0^L \gamma P(z) dz = \frac{2\pi}{\lambda A_{eff}} \int_0^L n_z P(z) dz, \tag{2}$$

where λ is the laser wavelength, A_{eff} is the fiber effective mode area, and n_2 is the nonlinear refractive index coefficient. When the B-integral exceeds approximately π, the nonlinear phase distortions become strong enough to degrade pulse compressibility, broaden the pulse duration, and introduce temporal pedestals. Controlling the B-integral is therefore essential for achieving high-quality compression at elevated output powers [14]:

To limit the growth of the nonlinear phase while maintaining efficient amplification, common strategies include increasing the mode field, shortening the effective length, reducing the peak power, and using a large-mode-area (LMA) Yb-doped fiber in the power amplifier. Its enlarged mode field reduces the nonlinear coefficient γ, allowing the system to operate at high power levels with a manageable B-integral. The tunable CFBG stretcher provides adjustable GDD and TOD, allowing the initial pulse chirp to be tailored to different amplification conditions. The stretcher, amplifier fiber, and compressor each contribute distinct amounts of second- and higher-order dispersion, and the interplay of these terms determines whether the SPM-induced chirp can be effectively removed during recompression. The resulting performance forms the basis for the experimental results presented in the following section.

3. Experimental Setup

The experimental system consists of a dispersion-controlled Yb-doped fiber chirped pulse amplifier (CPA) and a subsequent second-harmonic generation (SHG) module, designed to produce high-power, high-quality femtosecond pulses at 1030 nm and their frequency-doubled counterparts at 515 nm. The overall configuration is optimized to investigate how tunable dispersion pre-compensation enables stable pulse compression under power-dependent nonlinear phase accumulation. A schematic of the setup is shown in Figure 1.

The Yb-doped fiber CPA system provides dispersion-controlled amplification of femtosecond pulses. The front end consists of a Yb-doped fiber oscillator, a fiber preamplifier, a pulse picker, and a tunable CFBG (TPSR-T, TeraXion, Quebec, QC, Canada). The tunable CFBG selected directly follows from the need for tunable dispersion, providing adjustable GDD and TOD through controlling the mechanical strain and thermal tuning, modifying the effective grating period and refractive index distribution along the fiber. This tunability allowing the pre-chirp to be precisely controlled to counteract power-dependent nonlinear phase shifts accumulated during amplification, while maintaing low insert losses. Tunable CFBG provides a GDD of 13.6 ps^2 with a tuning range of 0.56 ps^2 and a TOD of -0.18 ps^3 with a tuning range of 0.036 ps^3. After stretching, the pulse duration increases to approximately 500 ps, with a central wavelength of 1034 nm and a spectral bandwidth of 12.5 nm,

as shown in Figure 2. The repetition rate of the system is 1 MHz, and the average output power of the front end is 41 mW. The CFBG effectively provides a required pre-chirp and dispersion control for the subsequent amplification and compression stages, and it can be recompressed to a pulse width of 249 fs, as shown in Figure 2c.

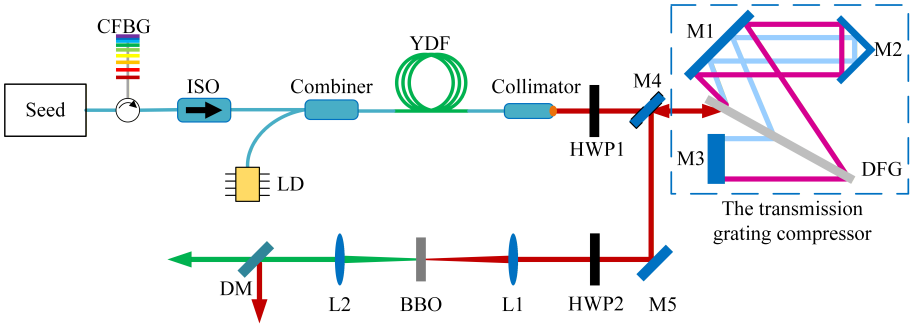


Figure 1. Schematic diagram of the experimental setup. CFBG: chirped fiber Bragg grating; ISO: isolator; LD: laser diode; YDF: Yb-doped fiber; HWP: half-wave plate; M1, M4, M5: 45° angle of incidence mirrors; M2: mirror pair for pulse compressor optical path horizontal folding; M3: mirror pair for pulse compressor optical path vertical folding; DFG: diffraction grating; DM: dichroic mirror. Different colored beams are used to distinguish the fundamental beam, different dispersion path inside the grating compressor, and the second-harmonic beam.

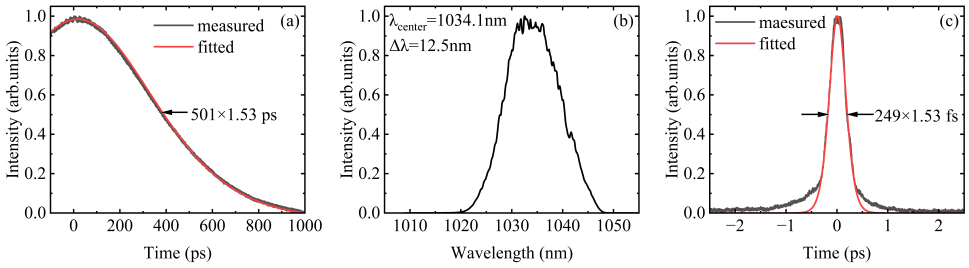


Figure 2. Output characteristics of the broadened pulse. (**a**) pulse duration of broadened pulse, (**b**) Spectrum of broadened pulse, (**c**) recompressed seed pulse duration.

Taking advantage of the high average power handling capabilities of large mode area fiber, we employ LMA Yb-doped double cladding fiber (PLMA-YDCF-25/250, Coherent, Bloomfield, CT, USA) with a 25 µm core diameter as the gain medium of the power amplifier, and a length of 1.8 m is chosen as a compromise between gain efficiency and nonlinear phase suppression. The amplifier is forward pumped by a multimode diode laser at 976 nm with maximum output power of 25 W. The gain fiber is coiled to 10 cm diameter to suppress high order modes, and a high-refractive-index coating adhesive is applied to absorb residual pump light at the fiber ends. The output power of the amplifier increases linearly with the increase of the pump power, and no power roll off is observed, as shown in Figure 3a. The estimated slope efficiency is 53.4% and maximum output power is 12.32 W, which is primarily limited by the available pump power while maintained excellent beam quality throughout operation.

After amplification, the pulses are directed into a specially designed and optimally adjusted compact single-grating transmission compressor including a large aperture diffraction grating, mirrors M1-M3 for folding the optical path, and M4 for guiding the beam through the compressor, as shown in Figure 1. The grating (Wasatch Photonics, Logan, UT, USA) has a groove density of 1700 lines/mm, and operates near the Littrow angle of 61.1° for vertical polarization, where diffraction efficiency is maximum. HWP1 is used to optimizing the input polarization to the required vertical state, achieving a diffraction efficiency above 95% per pass. The advantage of a single-grating transmission compressor is that

when the amount of dispersion needs to be adjusted, this can be achieved by moving the mirror M2 responsible for horizontal beam reflection or by slightly tilting the grating [15]. The compressor provides large negative GDD and large positive TOD to manage the cavity dispersion. The pulse experiences four passes through the grating before being reflected by mirror M4 and exiting the compressor. The compressed pulse average power reaches 9.65 W, corresponding to a compression efficiency of 78%, as shown in Figure 3b. The total optical loss of the system is dominated by the single transmission grating compressor, while the losses from lens and mirrors are negligible for high-reflection and high-transmittance coating; the experimental result is close to the theoretical value of 81%. The root mean square (RMS) power fluctuation of the compressed pulses is measured at the maximum output power over 30 min with a sampling interval of 1 s. As shown in Figure 3c, RMS fluctuation is 0.18%.

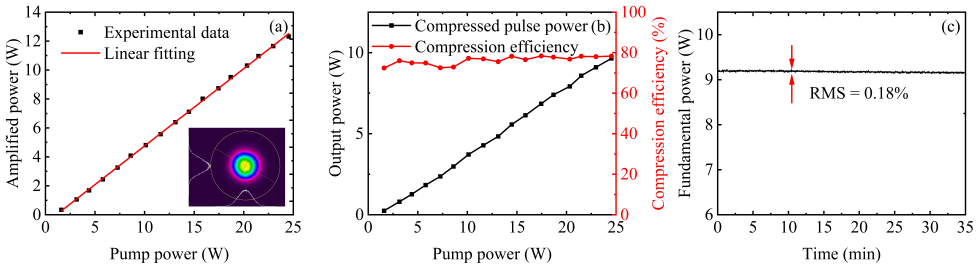


Figure 3. The amplification and compression performance versus the pump power. (**a**) Variation of 1030nm amplification power, inset: beam profile, (**b**) compressed pulse power with diode pump power, (**c**) power stability of the compressed pulse.

The compressed femtosecond pulses from the CPA system serve as the incident fundamental beam for the SHG stage. The frequency doubling is implemented using a type-I phase-matched beta-barium borate (BBO) crystal, chosen for its high nonlinear coefficient and wide transparency window [16]. The crystal has a thickness of 1 mm and a cutting angle of $\theta = 23.4°$, optimized for type-I (o + o $\rightarrow$ e) phase matching at the 1030 nm fundamental wavelength. HWP2 is used to adjust the incident fundamental beam polarization relative to the optical axis of the BBO crystal, thereby enabling efficient second-harmonic generation. The beam spatial profile characteristics are measured by a CCD spectrometer (SP620, Ophir Spiricon, Jerusalem, Israel), and its spectral properties are measured using an optical spectrum analyzer (AQ6373, Yokogawa, Tokyo, Japan) with a resolution of 0.05 nm. The corresponding pulse duration is deduced from the measured autocorrelation trace by an autocorrelator (PulseCheck, APE, Berlin, Germany) with sech2 fitting.

4. Results and Discussion

The total dispersion in the CPA system arises from three main components: the CFBG stretcher, the Yb-doped fiber amplifier and intracavity passive fiber, and the transmission grating compressor. The initial values of GDD and TOD of the stretcher are 13.56 ps² and -0.1791 ps³, respectively. The 4.5 m long fiber in the CPA system introduced a GDD of about 0.0989 ps² and TOD of about 0.189×10^{-4} ps³, respectively. In order to compensate the accumulated GDD and TOD introduced at the pre-stage, we theoretically calculated the incident angle of 60.6°, which is slightly apart from Littrow angle, together with an optical length of 27 cm between two grating passes, which provides a total amount of -13.73 ps² GDD and 0.1759 ps³ TOD [17]. In the experiment we fine-tuned the grating angle and M3 around theoretical values until the residual chirp was minimized. The interplay between these dispersive elements determines the net cavity dispersion of the system.

Figure 4 compares the temporal profiles of the compressed pulses under two different dispersion control strategies. The traces on Figure 4a are obtained by first optimizing the CFBG and grating separation at low power and then increasing the amplifier output without further dispersion adjustment. Under this condition, the pulse achieves a good autocorrelation waveform at 2.37 W and the pulse gradually broadens and develops temporal wings as the power increases. At the highest output of 9.65 W, the temporal waveform becomes significantly distorted with multiple satellite structures. This progressive degradation arises from the increasing nonlinear phase accumulation in the gain fiber.

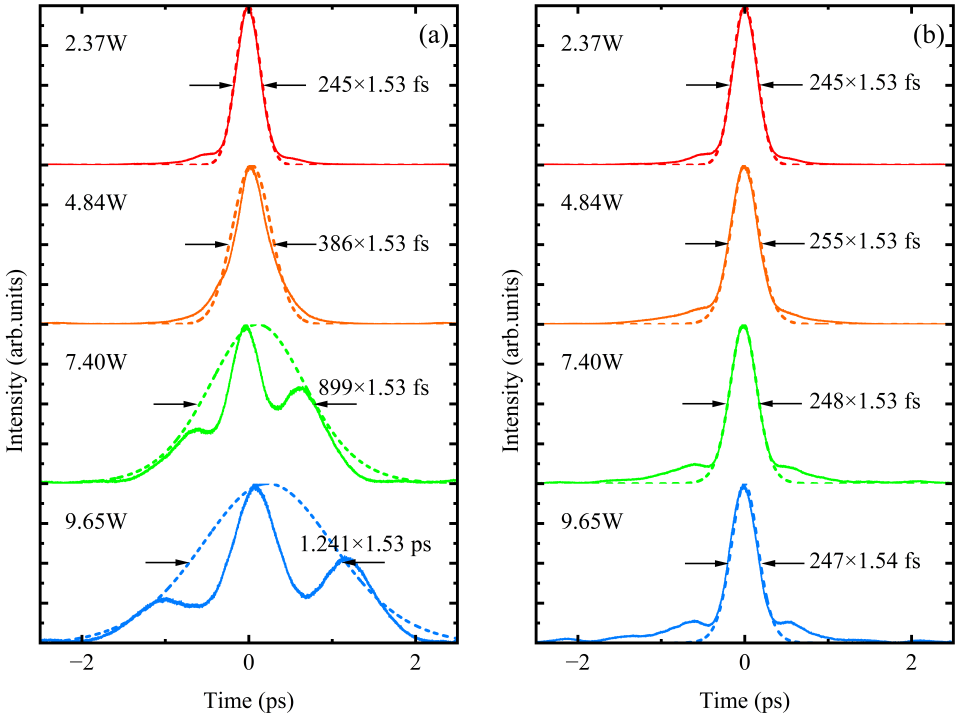


Figure 4. Autocorrelation traces of compressed pulse curves at different power levels (**a**) without and (**b**) with the fine-tuning of the dispersion of CFBG; the solid line measures autocorrelation trace, while the dashed line measures the sech2 fitting.

In contrast, Figure 4b shows the temporal traces obtained with a dynamic compensation strategy, where the CFBG is retuned at each power level to introduce an appropriate amount of additional negative TOD. In the experiment, the CFBG-provided TOD is adjusted from -0.1965 ps^3 at an output power of 2.37 W to -0.1791 ps^3 at an output power of 9.65 W. This adjustment effectively compensates the increasing nonlinear phase accumulation during amplification. Consequently, the pulses at the full operating power range compress to durations close to the minimum achievable value (250 fs), and the satellite structures observed in the fixed dispersion case are largely suppressed. By fine-tuning the pre-chirp of the CFBG, the total dispersion of the CPA chain is optimized to balance the nonlinear phase shift accumulated in the gain fiber. Under these conditions, appropriate dispersion pre-compensation effectively mitigates spectral distortion and temporal broadening induced by SPM, enabling stable pulse compression at high power levels.

The spectral changes at different output powers are shown in Figure 5, the approximate B integral can be given by assuming an exponential amplification [13,18], which is marked in the Figure 5a. With the output power increasing, the optical spectrum narrows, and its center wavelength shifts slightly toward shorter wavelengths, approaching the emission peak of the Yb-doped gain medium at 1030 nm. This spectral narrowing and blue shift are attributed to gain narrowing and nonlinear spectral reshaping within the fiber amplifier.

At the same time, although the B-integral increases, we do not observe a clear, monotonic SPM type spectral broadening that would normally be expected for strong self-phase modulation. Instead, the optical spectra exhibit multiple peaks, which are attributed to the combined effects of nonlinear spectral modulation induced by SPM, gain shaping of the Yb-doped fiber, and residual high-order dispersion. The small pedestal observed on the autocorrelation traces at higher powers arises from residual uncompensated higher-order dispersion and nonlinear phase modulation, which prevent the pulse from reaching the Fourier transform limit. Despite these effects, the recompressed pulses maintain good temporal quality, confirming that the dispersion tuning of the CFBG successfully compensates for power-dependent nonlinearities in the CPA chain.

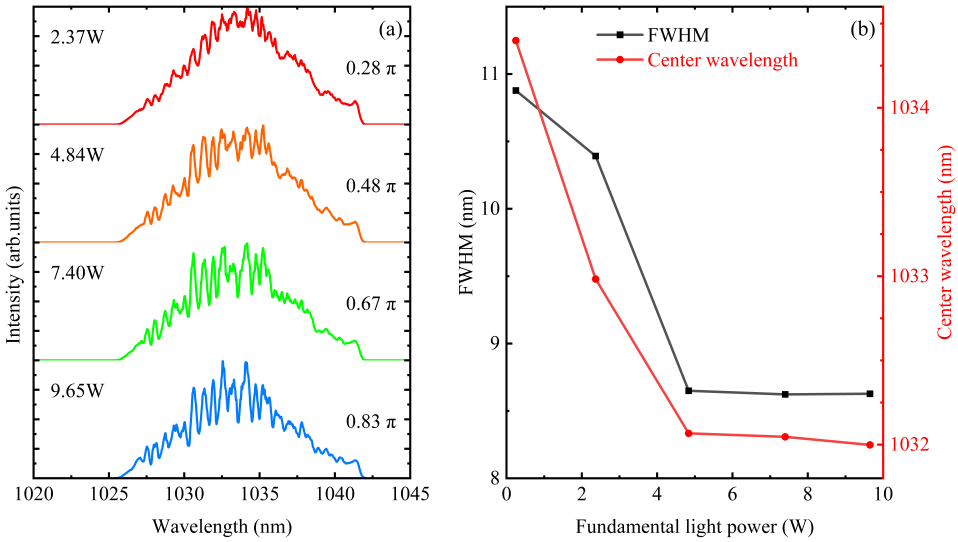


Figure 5. Spectral variations at different output powers. (**a**) Optical spectra of the compressed pulses at different output powers, (**b**) corresponding spectral evolution with increasing power.

The high-quality compressed pulses are used to drive the second-harmonic generation stage, with pulse durations individually optimized via tuning CFBG for each power level. The SHG light output power and conversion efficiency are measured as a function of the incident fundamental power, as shown in Figure 6a. The SHG power increases almost linearly at low incident power levels but gradually saturates, resulting in a slight decrease in conversion efficiency. The efficiency reduction may be due to phase mismatch caused by thermal effects in the BBO crystal at high average power. Despite these effects, the SHG process remains stable, demonstrating good power handling capability of the nonlinear stage. As shown in Figure 6b, the SHG power RMS stability at the highest output is 0.54% over 30 min, demonstrating an excellent stability of the system under peak operating conditions.

The temporal and spectral characteristics of the SHG pulses are shown in Figure 7. The measured second-harmonic spectra are centered at 517 nm with a full width at half maximum (FWHM) of approximately 2 nm. The measured pulse width at highest power output is 190 fs, exhibiting a small pedestal and closing to the Fourier transform limit of 144 fs. Since the SHG intensity is proportional to the square of the fundamental intensity in non-depleted regimes [19], significant uncompensated dispersion would have led to pronounced temporal broadening. The near transform-limited SHG pulse indicates that the residual spectral phase of the amplified 1030 nm femtosecond laser output is relatively small.

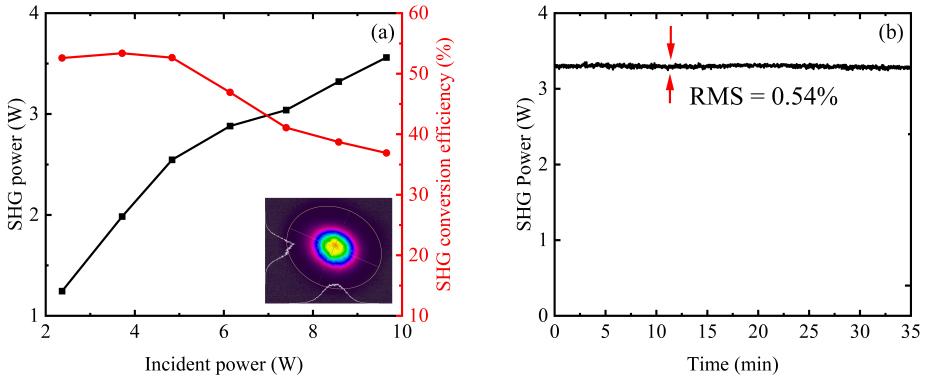


Figure 6. (**a**) SHG power (black curve, left axis) and SHG conversion efficiency (red curve, right axis) with different incident fundamental average power. Inset: beam profile. (**b**) Power surve of the SHG ligh for a duration of more than 30 min.

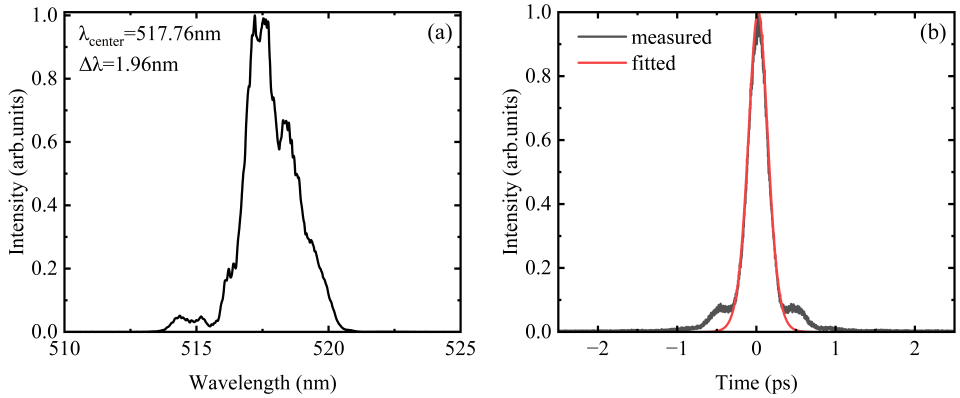


Figure 7. Output characteristics of the SHG pulse. (**a**) Spectrum of SHG pulse, (**b**) pulse duration of SHG pulse.

5. Conclusions

We have demonstrated a high-power Yb-doped fiber CPA system featuring tunable dispersion control via a CFBG stretcher. By dynamically adjusting GDD and TOD to match the nonlinear phase accumulated at different amplification powers, the CPA system achieves stable pulse compression over its full operating range. Importantly, the pulses maintain a nearly constant duration of 250 fs even at the maximum compressed power of 9.65 W, confirming that nonlinear distortions can be effectively compensated through adaptive dispersion management. The high-quality fundamental pulses further enable efficient SHG in a BBO crystal, yielding 3.56 W of 515 nm femtosecond output with near Fourier transform-limited temporal characteristics. The results demonstrate that combining managed nonlinearity with tunable dispersion offers a powerful and flexible strategy for scaling the performance of ultrafast fiber laser systems.

Author Contributions: Conceptualization, Z.Y., Q.W. and Y.F.; methodology: Q.W. and Y.F.; validation, Q.W. and Y.F.; investigation, Z.Y., Y.Z., B.Y. and N.W.; resources, Y.Q. and B.Y.; data curation, Z.Y., Y.Z. and M.Z.; writing—original draft preparation, Z.Y., Q.W. and Y.F.; writing—review and editing, Z.H., M.Z. and Y.W.; project administration, Y.F. and Y.Q.; funding acquisition, Y.F. All authors have read and agreed to the published version of the manuscript.

Funding: This work is supported by the Strategic Priority Research Program of the Chinese Academy of Sciences (Grant No. XDC 0240201).

Institutional Review Board Statement: Not applicable.

Informed Consent Statement: Not applicable.

Data Availability Statement: Data are contained within the article.

Conflicts of Interest: The authors declare no conflicts of interest.

References

1. Chang, G.; Wei, Z. Ultrafast fiber lasers: An expanding versatile toolbox. *iScience* **2020**, *23*, 101101. [CrossRef] [PubMed]
2. Donaldson, P.M.; Greetham, G.M.; Middleton, C.T.; Luther, B.M.; Zanni, M.T.; Hamm, P.; Krummel, A.T. Breaking barriers in ultrafast spectroscopy and imaging using 100 kHz amplified Yb-laser systems. *Accounts Chem. Res.* **2023**, *56*, 2062–2071. [CrossRef] [PubMed]
3. Wang, Z.; Wu, Y.; Qi, D.; Yu, W.; Zheng, H. Two-photon polymerization for fabrication of metalenses for diffraction-limited focusing and high-resolution imaging. *Opt. Laser Technol.* **2024**, *169*, 110128. [CrossRef]
4. Suda, A.; Takeda, T. Effects of nonlinear chirp on the self-phase modulation of ultrashort optical pulses. *Appl. Sci.* **2012**, *2*, 549–557. [CrossRef]
5. Saiyyed, R.; Sindhwani, M.; Sachdeva, S.; Pahuja, H.; Shukla, M.K. Comprehensive analysis of nonlinear effects in fiber optic communication systems: Exploring SPM, XPM, SS, and FWM. *J. Opt.* **2025**, 1–20. [CrossRef]
6. Ren, B.; Li, C.; Wang, T.; Guo, K.; Wu, J.; Su, R.; Ma, P.; Zhou, P. Generation of ultrafast laser with 11 MW peak power from a gain-managed nonlinear tapered fiber amplifier. *Opt. Laser Technol.* **2023**, *160*, 109081. [CrossRef]
7. Agrawal, G. *Nonlinear Fiber Optics*; Elsevier Science: Amsterdam, The Netherlands, 2013.
8. Zhou, S.; Kuznetsova, L.; Chong, A.; Wise, F.W. Compensation of nonlinear phase shifts with third-order dispersion in short-pulse fiber amplifiers. *Opt. Express* **2005**, *13*, 4869–4877. [CrossRef] [PubMed]
9. Song, H.; Liu, B.; Wen, L.; Wang, C.; Hu, M. Optimization of nonlinear compensation in a high-energy femtosecond fiber CPA system by negative TOD fiber. *IEEE Photonics J.* **2017**, *9*, 3200110. [CrossRef]
10. Lv, Z.G.; Teng, H.; Wang, L.N.; Wang, J.L.; Wei, Z.Y. High-energy femtosecond Yb-doped all-fiber monolithic chirped-pulse amplifier at repetition rate of 1 MHz. *Chin. Phys. B* **2016**, *25*, 094208. [CrossRef]
11. Wei, R.; Wang, M.; Zhu, Z.; Lai, W.; Yan, P.; Ruan, S.; Wang, J.; Sun, Z.; Hasan, T. High-power femtosecond pulse generation from an all-fiber Er-doped chirped pulse amplification system. *IEEE Photonics J.* **2020**, *12*, 3200208. [CrossRef]
12. Wang, T.; Li, C.; Ren, B.; Guo, K.; Wu, J.; Leng, J.; Zhou, P. High-power femtosecond laser generation from an all-fiber linearly polarized chirped pulse amplifier. *High Power Laser Sci. Eng.* **2023**, *11*, e25. [CrossRef]
13. Li, F.; Zhao, W.; Wang, Y.; Wang, N.; Li, Q.; Yang, Y.; Wen, W. A large dispersion-managed monolithic all-fiber chirped pulse amplification system for high-energy femtosecond laser generation. *Opt. Laser Technol.* **2022**, *147*, 107684. [CrossRef]
14. Li, Z.; Zhou, K.; Mu, J.; Zeng, X.; Wu, Z.; Wang, X.; Wang, X.; Zuo, Y. B-integral limitation of ultra-high-peak-power lasers. *High Power Laser Sci. Eng.* **2025**, *13*, e69. [CrossRef]
15. Bienert, F.; Graf, T.; Ahmed, M.A. Designing of grating pulse compressors. *Opt. Express* **2025**, *33*, 11500–11516. [CrossRef] [PubMed]
16. Hong, L.H.; Chen, B.Q.; Hu, C.Y.; Li, Z.Y. Spatial–temporal evolution of ultrashort laser pulse second harmonic generation in β-barium borate (β-BBO) crystal. *J. Appl. Phys.* **2021**, *129*, 233102. [CrossRef]
17. Chauhan, V.; Bowlan, P.; Cohen, J.; Trebino, R. Single-diffraction-grating and grism pulse compressors. *J. Opt. Soc. Am. B* **2010**, *27*, 619–624. [CrossRef]
18. Yu, H.; Wang, X.; Zhang, H.; Su, R.; Zhou, P.; Chen, J. Linearly-Polarized Fiber-Integrated Nonlinear CPA System for High-Average-Power Femtosecond Pulses Generation at 1.06. *J. Light. Technol.* **2016**, *34*, 4271–4277. [CrossRef]
19. Kim, G.; Yang, J.; Lee, B.; Sall', E.; Chizhov, S.; Kalintsev, A.; Yashin, V.; Kang, U. Efficient generation of the second and third harmonics of high-power femtosecond Yb: KGW-laser radiation in nonlinear-optical BBO crystals. *J. Opt. Technol.* **2016**, *83*, 463–467. [CrossRef]

Disclaimer/Publisher's Note: The statements, opinions and data contained in all publications are solely those of the individual author(s) and contributor(s) and not of MDPI and/or the editor(s). MDPI and/or the editor(s) disclaim responsibility for any injury to people or property resulting from any ideas, methods, instructions or products referred to in the content.